

Analytical Methods

Accepted Manuscript



This is an *Accepted Manuscript*, which has been through the Royal Society of Chemistry peer review process and has been accepted for publication.

Accepted Manuscripts are published online shortly after acceptance, before technical editing, formatting and proof reading. Using this free service, authors can make their results available to the community, in citable form, before we publish the edited article. We will replace this *Accepted Manuscript* with the edited and formatted *Advance Article* as soon as it is available.

You can find more information about *Accepted Manuscripts* in the [Information for Authors](#).

Please note that technical editing may introduce minor changes to the text and/or graphics, which may alter content. The journal's standard [Terms & Conditions](#) and the [Ethical guidelines](#) still apply. In no event shall the Royal Society of Chemistry be held responsible for any errors or omissions in this *Accepted Manuscript* or any consequences arising from the use of any information it contains.

Photoelectrochemical glucose biosensor in flow injection analysis system based on glucose dehydrogenase immobilized on poly-hematoxylin modified glassy carbon electrode

Didem Giray Dilgin^{a,b*}, H. İsmet Gökçel^b

^{a,b}Çanakkale Onsekiz Mart University, Biga Vocational School, Biga Çanakkale-Turkey

^bEge University, Science Faculty, Department of Chemistry, 35100 Bornova-İzmir, Turkey

Abstract

In this study, a photoelectrochemical glucose biosensor based on electropolymerized Hematoxylin film onto poly-amidoamine (PAMAM) dendrimers adsorbed glassy carbon electrode (Poly-HT/PAMAM/GCE) was presented. After the immobilization of glucose dehydrogenase (GDH) onto the poly-HT/PAMAM/GCE, photoelectrochemical biosensing of glucose was investigated using cyclic voltammetry and amperometry in flow injection analysis (FIA) system dependent on the NAD^+/NADH redox couple-dehydrogenase enzyme. The linear range was from 1×10^{-5} M to 1×10^{-3} M with the sensitivity of $0.76 \mu\text{AmM}^{-1}$ and detection limit of $3.0 \mu\text{M}$ without irradiation in FIA system. After the irradiation, the linear range was from 5×10^{-6} M to 1×10^{-3} M with the sensitivity of $1.90 \mu\text{AmM}^{-1}$ and a detection limit of $1.5 \mu\text{M}$. When the results obtained from the irradiation of electrode surface compared with the reaction without irradiation, the sensitivity and the detection limit increased around 2.5 and 2.0 folds, respectively. The photoelectrochemical biosensor showed a good performance with high upper detection limit, acceptable repeatability and selectivity providing a rapid alternative method for monitoring biomolecules and extending the photoelectrochemical determination in FIA system. The proposed electrochemical and photoelectrochemical biosensor was successfully applied to determination of glucose in real samples. It was indicated that the results obtained from this study will provide the basis for a further development for future studies in these directions.

Keywords: Photoelectrochemical biosensor, flow injection analysis, hematoxylin, NADH, glucose dehydrogenase.

*Corresponding Author

E-mail: didemgiray79@hotmail.com

1. Introduction

Chemically Modified Electrodes (CMEs) have attracted considerable attention in the development of new electrochemical sensors and biosensors, because CMEs offer advantages such as high sensitivity, selectivity, reduced interference effect, preconcentration of target species, etc.¹⁻³ An important application area of CMEs is investigation of electrocatalytic oxidation of Reduced β -Nicotinamide adenine dinucleotide (NADH) and construction of biosensors for some biologically important compounds that depend on NAD^+/NADH redox couple and dehydrogenase enzymes⁴⁻⁷. The biosensing of molecules using dehydrogenase enzymes requires a highly sensitive NADH transducer, because the transformed signal of the biosensor is based on the detection of enzymatically generated NADH.

However, direct electrochemical oxidation of NADH to NAD^+ ; at the bare electrode surface is highly irreversible and takes place at high overpotential (between 0.5 and 1 V dependent on electrode type) and is accompanied by rapid poisoning of the reaction because the electrode surface is fouled by adsorption of its oxidation products and intermediate radicals^{4,8}. In order to overcome these problems, modification of the electrode surface with redox mediators has been extensively used. Various modified electrodes have been prepared with many redox mediators such as azine type dyes (phenothiazine, phenoxazine, phenazine), quinolic compounds (flavonoids, phenolic acids, catecholic compounds), nitrofluorenones, flavine and adenine derivatives, some transition metal complexes and some conducting polymers⁴⁻⁶. Modified electrodes prepared with various redox mediators have also been used for the construction of electrochemical biosensors for many biologically important molecules based on dehydrogenase enzymes^{6,9-13}.

Recently, many scientists have focused on photoelectrochemical sensors, which are a newly developed analytical device based on the photoelectrochemical properties of electrode or mediators. Because the combination of CMEs and photoelectrochemistry exhibits more sensitive results than that of CMEs without irradiation electrode surface. Poly-Toluidine Blue (poly-TB)¹⁴, poly-Methylene Blue (poly-MB)¹⁵, poly-Hematoxylin (Poly-HT)¹⁶, poly-Neutral Red (Poly-NR)¹⁷ modified glassy carbon electrodes (GCE), a new polymeric phenothiazine modified graphite electrode¹⁸, Graphene-TiO₂ nanohybrids modified GCE¹⁹, Dopamine/nanoporous TiO₂ modified Indium Tin Oxide (ITO) electrode²⁰, and poly(4,4'-diaminodiphenyl sulfone)/nanoTiO₂ composite film ITO electrode²¹ have been used for the photoelectrocatalytic oxidation of NADH. In these studies, a significant enhancement in the current for the oxidation of NADH was observed when the working electrode surface was

1
2
3 irradiated by a light source. In addition, a photoelectrochemical glucose biosensor based on
4 NAD^+/NADH redox couple and glucose dehydrogenase enzyme has been constructed by
5 using the Quantum dot modified Au electrode²² and Thionine (Th) cross-linked multi-walled
6 carbon nanotubes (MWNTs) and Au nanoparticles (Au NPs) multilayer functionalized ITO
7 electrode²³. These studies showed that the sensitivity of a photoelectrochemical sensor was
8 better than an electrochemical sensor.
9

10
11
12
13 Another useful approach in electrochemical sensors and biosensors is the usage of Flow
14 Injection Analysis (FIA) with CMEs in electrochemical techniques^{24,25}. Because FIA has
15 some advantages for routine analytical determinations such as very limited sample
16 consumption, short analysis time based on a transient signal measurement in a flow-through
17 detector, and an on-line carrying out difficult operations of separation, chemical conversion of
18 analyses into detectable species. Electrocatalytic oxidation of NADH and biosensors that
19 depend on NAD^+/NADH redox couple-dehydrogenase enzymes has also been investigated in
20 FIA with redox mediator-modified electrodes^{15,16,26-30}.
21

22
23
24
25
26 It is concluded that the combination of CMEs, photoelectrochemistry and FIA can be
27 useful for electrocatalytic oxidation of NADH and biosensor dependent on NAD^+/NADH
28 redox couple-dehydrogenase enzyme. When we take into consideration the advantages of this
29 combination, the developed photoelectrochemical sensor and biosensor offers advantages
30 such as i) good selectivity (CMEs have good selectivity properties), ii) good sensitivity (the
31 sensitivity of photoelectrochemical sensors is generally better than electrochemical sensors),
32 and iii) fast and economical analysis (FIA exhibits fast analysis and lower cost due to less
33 consumption of reactive). Therefore, an investigation on photoelectrocatalytic oxidation of
34 NADH and the construction of photoelectrochemical glucose biosensor dependent on
35 NAD^+/NADH redox couple-glucose dehydrogenase enzyme in the FIA system have been
36 proposed using glucose dehydrogenase immobilized on poly-Hematoxylin modified glassy
37 carbon electrode in this study.
38
39
40
41
42
43
44
45
46

47 **2. Results and Discussion**

48 **2.1. Electropolymerization of HT on PAMAM/GCE surface**

49
50
51
52
53
54
55
56
57
58
59
60
61
62
63
64
65
66
67
68
69
70
71
72
73
74
75
76
77
78
79
80
81
82
83
84
85
86
87
88
89
90
91
92
93
94
95
96
97
98
99
100
101
102
103
104
105
106
107
108
109
110
111
112
113
114
115
116
117
118
119
120
121
122
123
124
125
126
127
128
129
130
131
132
133
134
135
136
137
138
139
140
141
142
143
144
145
146
147
148
149
150
151
152
153
154
155
156
157
158
159
160
161
162
163
164
165
166
167
168
169
170
171
172
173
174
175
176
177
178
179
180
181
182
183
184
185
186
187
188
189
190
191
192
193
194
195
196
197
198
199
200
201
202
203
204
205
206
207
208
209
210
211
212
213
214
215
216
217
218
219
220
221
222
223
224
225
226
227
228
229
230
231
232
233
234
235
236
237
238
239
240
241
242
243
244
245
246
247
248
249
250
251
252
253
254
255
256
257
258
259
260
261
262
263
264
265
266
267
268
269
270
271
272
273
274
275
276
277
278
279
280
281
282
283
284
285
286
287
288
289
290
291
292
293
294
295
296
297
298
299
300
301
302
303
304
305
306
307
308
309
310
311
312
313
314
315
316
317
318
319
320
321
322
323
324
325
326
327
328
329
330
331
332
333
334
335
336
337
338
339
340
341
342
343
344
345
346
347
348
349
350
351
352
353
354
355
356
357
358
359
360
361
362
363
364
365
366
367
368
369
370
371
372
373
374
375
376
377
378
379
380
381
382
383
384
385
386
387
388
389
390
391
392
393
394
395
396
397
398
399
400
401
402
403
404
405
406
407
408
409
410
411
412
413
414
415
416
417
418
419
420
421
422
423
424
425
426
427
428
429
430
431
432
433
434
435
436
437
438
439
440
441
442
443
444
445
446
447
448
449
450
451
452
453
454
455
456
457
458
459
460
461
462
463
464
465
466
467
468
469
470
471
472
473
474
475
476
477
478
479
480
481
482
483
484
485
486
487
488
489
490
491
492
493
494
495
496
497
498
499
500
501
502
503
504
505
506
507
508
509
510
511
512
513
514
515
516
517
518
519
520
521
522
523
524
525
526
527
528
529
530
531
532
533
534
535
536
537
538
539
540
541
542
543
544
545
546
547
548
549
550
551
552
553
554
555
556
557
558
559
560
561
562
563
564
565
566
567
568
569
570
571
572
573
574
575
576
577
578
579
580
581
582
583
584
585
586
587
588
589
590
591
592
593
594
595
596
597
598
599
600
601
602
603
604
605
606
607
608
609
610
611
612
613
614
615
616
617
618
619
620
621
622
623
624
625
626
627
628
629
630
631
632
633
634
635
636
637
638
639
640
641
642
643
644
645
646
647
648
649
650
651
652
653
654
655
656
657
658
659
660
661
662
663
664
665
666
667
668
669
670
671
672
673
674
675
676
677
678
679
680
681
682
683
684
685
686
687
688
689
690
691
692
693
694
695
696
697
698
699
700
701
702
703
704
705
706
707
708
709
710
711
712
713
714
715
716
717
718
719
720
721
722
723
724
725
726
727
728
729
730
731
732
733
734
735
736
737
738
739
740
741
742
743
744
745
746
747
748
749
750
751
752
753
754
755
756
757
758
759
760
761
762
763
764
765
766
767
768
769
770
771
772
773
774
775
776
777
778
779
780
781
782
783
784
785
786
787
788
789
790
791
792
793
794
795
796
797
798
799
800
801
802
803
804
805
806
807
808
809
810
811
812
813
814
815
816
817
818
819
820
821
822
823
824
825
826
827
828
829
830
831
832
833
834
835
836
837
838
839
840
841
842
843
844
845
846
847
848
849
850
851
852
853
854
855
856
857
858
859
860
861
862
863
864
865
866
867
868
869
870
871
872
873
874
875
876
877
878
879
880
881
882
883
884
885
886
887
888
889
890
891
892
893
894
895
896
897
898
899
900
901
902
903
904
905
906
907
908
909
910
911
912
913
914
915
916
917
918
919
920
921
922
923
924
925
926
927
928
929
930
931
932
933
934
935
936
937
938
939
940
941
942
943
944
945
946
947
948
949
950
951
952
953
954
955
956
957
958
959
960
961
962
963
964
965
966
967
968
969
970
971
972
973
974
975
976
977
978
979
980
981
982
983
984
985
986
987
988
989
990
991
992
993
994
995
996
997
998
999
1000

Prior to enzyme immobilization, redox mediator HT, which shows a good electrocatalytic and also photoelectrocatalytic effect towards the oxidation of NADH^{16} was electropolymerized onto PAMAM/GCE. Figure 1 shows the typical cyclic voltammograms of

1
2
3 the polymer film growth during the electropolymerization of 0.3 mM HT solution in 0.1 M
4 phosphate buffer solution (PBS, pH 7.0) containing 0.1 M NaNO₃. NaNO₃ was used as 0.1 M
5 in the supporting electrolyte during all the electropolymerization process due to the catalytic
6 effect of the NO₃⁻ anions on the electropolymerization process³¹. In the first cycle of cyclic
7 voltammograms of HT (Fig.1, black line), one oxidation peak was observed at about 385 mV
8 with a shoulder at 285 mV, which is attributed to the oxidation of monomeric catechol groups
9 to quinone. The reduction peak was also formed more specifically at about -480 mV. In the
10 second cycle, the oxidation peak current decreased. After the third cycle, the oxidation peak
11 current began to grow slowly with increasing cycle numbers and peak potential was shifted to
12 about 310 mV. Cathodic peak of HT at about -480 mV increased gradually with increasing
13 scan cycles (Fig. 1). These results demonstrated that the polymeric film of HT could be formed
14 on GCE. In our previous study¹⁶, similar discussions and electropolymerization mechanism
15 was reported for electropolymerization of HT on GCE. The electropolymerized HT film was
16 also prepared on GCE at the same conditions (data not shown). However, it was observed that
17 increase of monomeric peaks by increasing the scan cycle at PAMAM/GCE was found to be
18 better than at GCE. This result shows that PAMAM dendrimer has a good surface for
19 electropolymerization of HT.
20
21
22
23
24
25
26
27
28
29
30
31
32

33 **Fig. 1**

34 **2.2. Cyclic voltammetric studies for photoelectrochemical biosensing of glucose**

35
36
37
38
39
40 Electrochemical and photoelectrocatalytic oxidation of glucose at GDH based poly-HT
41 modified GCEs were investigated using cyclic voltammetric techniques. Firstly, the
42 electrochemical and photoelectrochemical response of dehydrogenase immobilized PAMAM
43 modified GCE (GDH/PAMAM/GCE without poly-HT) to glucose was investigated by
44 recording cyclic voltammograms. For this, cyclic voltammograms of GDH/PAMAM/GCE
45 were recorded in 0.1 M PBS (pH 7.0) containing 10 mM NAD⁺ in the absence and in the
46 presence of 10 mM glucose at 5 mV s⁻¹ scan rate, respectively. The obtained cyclic
47 voltammograms are given in Figure 2A. In the first voltammograms (Fig. 2A/a), no peak was
48 observed because the supporting electrolyte did not include any substrate (glucose). When the
49 substrate was added to supporting electrolyte, a reversible peak at about 760 mV at
50 GDH/PAMAM/GCE (Fig. 2A/b) was observed, which was attributed to the oxidation of
51 enzymatically produced NADH to NAD⁺ at PAMAM modified GCEs (Reactions 1 and 2).
52
53
54
55
56
57
58
59
60

When the electrode surface was irradiated with the light source, the peak current increased a little (Fig. 2A/c).

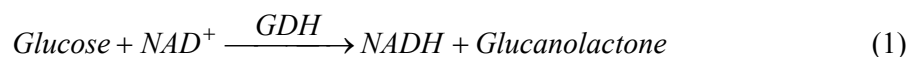
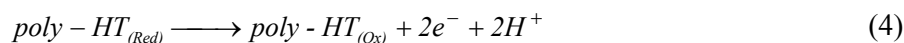
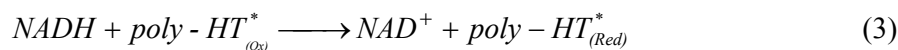


Fig. 2

After polymerization of HT, GDH was immobilized onto poly-HT/PAMAM/GCE. The electrochemical and photoelectrochemical response of GDH/Poly-HT/PAMAM/GCE to glucose was also investigated by cyclic voltammetric technique. The above mentioned (for GDH/PAMAM/GCE) cyclic voltammetric procedures for biosensing and photobiosensing of glucose were also repeated for this electrode. The obtained cyclic voltammograms are given in Figure 2B. In the first cyclic voltammogram, only an anodic peak at about 210 mV with a shoulder at 120 mV was observed in the presence of NAD^+ (Fig. 2B/a). These peaks can be attributed to oxidation of polymeric form of HT. In the presence of glucose, the current of this peak increased, which is attributed to the electrocatalytic oxidation of enzymatically produced NADH to NAD^+ (Fig. 2B/b). When the electrode surface was irradiated with the light source, a large enhancement in this peak current was observed (Fig. 2B/c). If it was compared the peak potential of glucose at GDH/PAMAM/GCE (about 760 mV, see Figure 2A/b) with that at the GDH/poly-HT/PAMAM/GCE (about 300 mV, Fig. 2B/b), the overpotential for the electrochemical oxidation of NADH produced by enzymatic reaction of glucose decreased by 460 mV at GDH/poly-HT/PAMAM/GCE. Moreover, the peak current at 300 mV (GDH/poly-HT/PAMAM/GCE) attributed to electrocatalytic oxidation of NADH increased with irradiation of electrode surface (Fig. 2B/c). The increase in the electrocatalytic peak current of NADH with light depends on excitation of poly-HT on the electrode surface and its excited form can more rapidly react with NADH. Thus, it can be concluded that irradiation of the surface of GDH/ poly-HT/PAMAM/GCE causes a faster photoelectrochemical oxidation of NADH than that of electrochemical. The mechanism can be explained by reactions between 1 and 4. According to equation 4, the increasing oxidation current of poly HT(red) which was produced dependent on the concentration of enzymatically produced NADH was observed upon illumination. However, in the cyclic voltammograms of GDH/poly-HT/PAMAM/GCE in the presence of 10 mM NAD^+ with irradiation of electrode surface, a small enhancement on peak current of HT was observed (see supplementary file, Figure S1), indicating that a big

enhancement on peak current in the presence of glucose is dependent on NADH (indirectly glucose) concentration.



These results showed that the photoelectrochemical biosensor dependent on $NAD^+/NADH$ redox couple and dehydrogenase enzyme can be constructed for glucose detection. A similar result was also obtained for Thionine modified multiwalled carbon nanotube and gold nanoparticles functionalized indium tin oxide electrode²³. However, in this cited study FIA system was not used. As distinct from this, the proposed method in present study also includes photoelectrochemical biosensor in FIA system.

2.3. Photoamperometric detection of glucose in FIA system

2.3.1. Optimization of the Experimental Parameters

After the investigation of electrochemical and photoelectrochemical biosensing of glucose using cyclic voltammetric technique, it was also investigated using amperometric techniques in FIA system. In order to obtain the best amperometric and photoamperometric response of GDH/Poly-HT/PAMAM/GCE towards glucose in FIA system, the effect of the applied potential and flow rate on the current of 0.8 mM glucose containing 10 mM NAD^+ was investigated by recording diagrams. Firstly, the applied potential was optimized under the conditions of 1.1 mL min^{-1} flow rate, 100 μL sample loop, 10 cm tubing length and 0.1 M PBS (pH 7.0) containing 0.1 M KCl as carrier stream. Then, the current-time curves were recorded at various applied potential. After a steady background current was obtained, 0.8 mM glucose containing 10 mM NAD^+ was injected into the carrier stream. The amperometric and photoamperometric currents were measured from current-time curves obtained at various applied potential. The current-time curves of GDH/Poly-HT/PAMAM/GCE for 0.8 mM glucose containing 10 mM NAD^+ obtained at various applied potential were shown in Figure S2/A (see supplementary file). In addition, Figure S2/B (see supplementary file) shows the plot of electrocatalytic and photoelectrocatalytic currents of glucose versus the applied potential. The best currents for electrocatalytic and photoelectrocatalytic oxidation of NADH produced by

enzymatic reaction of glucose in FIA system were found at about 300 mV. In addition, the current values obtained from the photoamperometric method were about 50-40% higher than that obtained from amperometric method. Thus an applied potential of 300 mV was selected as optimum in order to minimize interference effects.

In the second optimization step, the effect of flow rate on electrocatalytic and photoelectrocatalytic currents of glucose was investigated. For this purpose, the current-time curves were recorded at various flow rates using GDH/Poly-HT/PAMAM/GCE in 0.1 M PBS (pH 7.0) containing 0.1 M KCl using 100 μ L sample loop and 10 cm tubing length. In these conditions, the obtained diagrams for 0.8 mM glucose containing 10 mM NAD^+ at various flow rates were shown in Figure S3/A shows and the plot of the electrocatalytic and photoelectrocatalytic currents versus flow rate were shown in Figure S3/B (see supplementary file).

As can be seen in these figures, the maximum peak current was observed at the lowest flow rate, 0.125 mL, because, biosensors and photoelectrochemical biosensors could find enough time for the occurrence of enzymatic reaction and also photoexcitation of mediator in the low flow rate. The peak currents decreased by increasing the flow rate from 0.125 mL min^{-1} to 2.2 mL min^{-1} . Thus, the lowest flow rate, 0.125 mL min^{-1} was selected as optimum flow rate even though sample frequency is very low.

2.3.2. Calibration curve and amperometric response in FIA

To establish that a reliable analytical response could be achieved for the glucose, under optimized conditions using a GDH/Poly-HT/PAMAM/GCE, a calibration study was carried out over the range 5×10^{-6} – 1×10^{-2} M glucose concentration, with two injections of each concentration being made via a 100 μ L sample loop. Figure 3 shows the diagrams for amperometric and photoamperometric FI responses to various concentrations of glucose. Although the peak currents increased depending on glucose concentration for both the amperometric and the photoamperometric methods, the responses of photoamperometric method were higher than those of amperometric in all concentrations.

Both amperometric and photoamperometric currents at various concentrations of glucose were also recorded using GDH/PAMAM/GCE (without HT) in the optimized conditions. Figure S4 (see supplementary file) shows current-time curves obtained from GDH/PAMAM/GCE for various glucose concentrations. No enzymatically produced NADH

oxidation peaks were observed until 8 mM glucose concentration. Only small peaks were observed up to 8 mM glucose. Thus, it can be concluded that the using of electropolymerization of HT in the electrode modification emphasizes its importance in especially photoamperometric measurements.

Fig. 3

Figure 4A shows a plot of catalytic current versus glucose concentration. From this figure, a linear relationship between the glucose concentration and the peak current was obtained over the concentration range $1 \times 10^{-5} - 1 \times 10^{-3}$ M and $5 \times 10^{-6} - 1 \times 10^{-3}$ M by the amperometric FIA and the photoamperometric FIA method, respectively, at the GDH/Poly-HT/PAMAM/GCE (Figure 4B). The linearity of these methods is described by the following equations:

$$i (\mu\text{A}) = 0.76c (\text{mM}) + 0.0035 \quad (R^2 = 0.995)$$

$$i (\mu\text{A}) = 1.90c (\text{mM}) + 0.0027 \quad (R^2 = 0.998)$$

for amperometric and photoamperometric studies, respectively, where i is the peak current and c is the concentration of glucose. When these equations are compared in terms of their slopes, it is clear that the sensitivity of the photoelectrocatalytic FIA procedure is better than that of the amperometric method and the ratio of improvement is about 2.5. The limit of detection (LOD) was calculated as 3×10^{-6} and 1.5×10^{-6} M glucose for amperometric and photoamperometric glucose biosensors, respectively, based on $3s_b/m$ where s_b is the standard deviation of the blank response and m is the slope of the calibration curve. Limit of quantification (LOQ) was calculated as 1×10^{-5} and 5×10^{-6} M glucose for amperometric and photoamperometric glucose biosensors, respectively, based on $10s_b/m$.

Fig. 4

The precision of electrochemical and photoelectrochemical biosensor was investigated by making 5 repeat injections of 3×10^{-4} and 1×10^{-3} M glucose solution. The RSD for electrochemical and photoelectrochemical biosensors were calculated to be 1.8% and 2.3% for 3.0×10^{-4} and 1.4% and 3.5% for 1×10^{-3} M, respectively. These results indicate GDH/Poly-HT/PAMAM/GCE has very good repeatability for electrochemical and photoelectrochemical biosensing of glucose.

1
2
3 The apparent Michaelis–Menten constant K_m , which depicts the enzyme-substrate
4 kinetics of biosensor, can be calculated from the Lineweaver–Burk equation: $1/I_{ss} =$
5 $(K_m/I_{max})(1/C_s) + 1/I_{max}$, where C_s is the substrate concentration, I_{ss} is the steady-state current
6 and I_{max} is the maximum current measured under substrate saturation³². From the curve of the
7 I_{ss}^{-1} versus C_s^{-1} (see supplementary file, Figure S5), based on the experimental data from Fig.
8 4A, the apparent Michaelis–Menten constant K_m and the maximum current response I_{max} were
9 estimated to be 1.12 mM, 3.5 $\mu\text{A}/\text{mM}$ for amperometric method and 4.4 mM, 5.13 $\mu\text{A}/\text{mM}$
10 for amperometric method, respectively. The value of K_m agrees well with the reported value
11 of K_m for GDH modified electrodes for example 1.767 mM for carbon nanotube-ionic liquid-
12 chitosan-GDH modified GCE³³ is much lower than the reported values of K_m for some
13 constructed biosensors (4.53 and 3.09³⁴, 12³⁵ and 6.7³⁶ mM) dependent on GDG and
14 NAD^+/NADH redox couple. Smaller K_m values show that the electrochemical and
15 photoelectrochemical biosensors possess higher biological affinity to glucose and have a
16 superior enzymatic activity.
17
18
19
20
21
22
23
24
25
26
27

28 2.3.3. Investigation of interfering substances

29
30
31 There are various species that interfere with glucose detection in the real samples,
32 including ascorbic acid (AA), dopamine (DA), uric acid (UA), L-cysteine (L-Cyst) and other
33 monosaccharides such as galactose, saccharose, and fructose. With this aim, the diagrams of
34 glucose in the presence of these interfering compounds without irradiation were recorded in
35 the optimum conditions. Figure S6 (see supplementary file) shows the obtained diagram of
36 3×10^{-4} M glucose in the presence of possible interfering compounds with various
37 concentrations. As can be seen, in the presence of AA, DA, UA and L-Cyst, serious
38 interferences were occurred with the amperometric enzyme glucose sensors because their
39 oxidation potentials were close to that of glucose (300 mV at GDH/Poly-HT/PAMAM/GCE).
40 It was generally reported that, using the Nafion membrane effectively removes the
41 interference of AA because it is negatively charged and repels negatively charged organic
42 species³⁷. However, it is difficult to remove the interference caused by neutral or positively
43 charged, very small organics, such as DA and UA, etc. Consequently, these interfering species
44 cannot be removed using only a Nafion membrane. Another possible way to eliminate the
45 interference effect of AA, is to use ascorbate oxidase³⁸. While ascorbate is selectively
46 oxidized to dehydroascorbate in the presence of ascorbate oxidase and molecular oxygen,
47 NADH produced by enzymatic reaction was not influenced by this medium.
48
49
50
51
52
53
54
55
56
57
58
59
60

1
2
3 In order to remove the interfering effect of these compounds, very small amount of
4 lead(IV) acetate as an oxidizing agent can be added to Nafion layer due to preoxidation
5 reaction of these interfering compounds before they reach the electrode surface³⁷.
6
7

8 On the other hand, no interference in the presence of other monosaccharides including
9 galactose, saccharose and fructose was observed because the GDH is very selective for
10 glucose against other monosaccharides. In order to reduce the interfering effect of AA, DA,
11 UA and L-Cyst, the fiagrams of 3×10^{-4} M glucose were also recorded in the absence and in the
12 presence of these interfering compounds at applied potential of 100 mV. Although
13 interference effect of UA and L-Cyst was reduced, the reducing of interfering effect of AA
14 and DA has not been achieved in this potential also. On the other hand, the peak current of
15 glucose at 100 mV decreased about two folds in comparison with 300 mV.
16
17
18
19
20
21
22

23 **2.3.4. Storage stability of the biosensor**

24
25
26 The storage stability of the biosensor has been studied over a period of 15 days. The
27 sensor was stored in 0.1 M PBS (pH 7.0) at 4°C when not in use. The electrocatalytic and
28 photoelectrocatalytic current responses could maintain about 85% and 50% of the initial signal,
29 respectively. The first reason of decrease in photoelectrochemical biosensor responses was the
30 effect of light on dehydrogenase enzyme. The other reason was defects and deformations
31 occurring on modified electrodes day by day.
32
33
34
35
36
37

38 **2.3.5. Real sample analysis**

39
40
41 In order to show the practical applicability of the proposed biosensor, two real samples
42 (human blood serum and commercial dextrose solution) were selected for determination of
43 glucose as described in literature³⁹. 250 μ L of blood serum samples were diluted to 5 mL with
44 0.1 M PBS (pH 7.0) containing 10 mM NAD⁺ and 1 M KCl. Glucose detection was
45 performed by spiking a known volume and concentration of glucose standard solution into the
46 diluted serum samples in order to obtain various concentrations, and by measuring of the
47 amperometric and photoamperometric response of electrode in FIA system. Commercially
48 supplied dextrose solution (including 5% glucose) was used as a second real sample. For the
49 determination of glucose, dextrose solution was diluted 555 times with 0.1 M PBS (pH 7.0)
50 containing 10 mM NAD⁺ and 1 M KCl. Thus diluted dextrose solution containing about 0.5
51 mM glucose was obtained. Glucose detection was also performed for this sample as described
52
53
54
55
56
57
58
59
60

1
2
3 human serum sample. The results for the recovery test were given in Table 1. It can be seen
4 that acceptable recoveries were obtained for spiked glucose in blood plasma and commercial
5 dextrose solution samples.
6
7

8 9 **3. Experimental**

10 11 12 **3.1. Apparatus**

13
14
15
16 Cyclic voltammetric and chronoamperometric measurements were performed at room
17 temperature in a traditional three electrode system. A platinum wire was used as the counter
18 electrode, an home-made Ag/AgCl (saturated KCl) electrode as the reference electrode and a
19 PTFE-shrouded GCE (MF2040 Bioanalytical system, 3 mm diameter) as the working
20 electrode. However, an Ag/AgCl (0.1 M KCl) was used as reference electrode for the
21 chronoamperometric measurements in FIA system. All electrochemical experiments were
22 carried out using two voltammetric instruments, Compactstat Electrochemical Interface
23 (Ivium Technologies, Eindhoven, Netherlands) and Autolab PGSTAT302N
24 Potentiostat/Galvanostat. In order to record cyclic voltammograms during
25 photoelectrochemical experiments, a fiberoptic illuminator 250 W halogen bulb with Foi-5
26 Light Guide (Titan Tool Supply Inc., USA) was used to irradiate the electrode surface within
27 a home-made photoelectrochemical cell, which was constructed of Teflon¹⁶. A Perkin Elmer
28 Lambda 35 Uv-Vis Spectrometer was used for measuring the absorbance of the NADH
29 solutions at 340 nm. . The pH of the buffer solutions was measured using a Hanna HI 221 pH-
30 meter with a combined glass electrode (Hanna HI 1332). A Bandelin Sonorex RK 100H
31 Ultrasonic bath was used for cleaning procedure of the GCEs before their modification.
32 Deionized water supplied by a Milli-Q device (Millipore, Bedford, USA) throughout all
33 experiments. In order to perform FIA experiments, an eight-channel Ismatec, Ecoline
34 peristaltic pump with polyethylene tubing (0.75mm i.d.), and a Rheodyne 8125 sample
35 injection valve were used.
36
37
38
39
40
41
42
43
44
45
46
47
48
49

50 51 **3.2. Chemicals**

52
53
54 Glucose dehydrogenase enzyme from *Pseudomonas* sp. (GDH, 338.7 U/mg), β -
55 Nicotinamide adenine dinucleotide sodium salt from *saccharomyces cerevisiae*
56 ($C_{21}H_{26}N_7NaO_{14}P_2$, $NaNAD^+$, MW: 685.41 g mol⁻¹), Bovine serum albumin (BSA),
57
58
59
60

1
2
3 glutaraldehyde (GA, d: 1.061 g mL⁻¹, MW: 100.12 g mol⁻¹, 25% w/w in water) and PAMAM
4 Dendrimer, ethylenediamine core, generation 4.0 (d: 0.813 g mL⁻¹, MW: 14214.17 g mol⁻¹,
5 10% w/w in methanol) were supplied from Sigma-Aldrich (St. Louis, USA). D-Glucose,
6 Reduced β -Nicotinamide adenine dinucleotide, disodium salt (MW: 709.40 g mol⁻¹
7 C₂₁H₂₇N₇Na₂O₁₄P₂, NADHNa₂), Hematoxylin, (HT, C₆H₁₄O₆,) were supplied from Merck
8 (Steinheim, Germany). Other used chemicals such as HNO₃ (65%, 1.39 g mL⁻¹), HCl (30%,
9 1.15 g mL⁻¹), H₃PO₄ (85%, 1.71 g mL⁻¹) KCl, NaH₂PO₄·2H₂O, Na₂HPO₄·2H₂O, NaOH,
10 NaNO₃, methanol and ethanol were purchased from Merck or Sigma-Aldrich Companies and
11 they were also of analytical reagent grade.
12
13
14
15
16
17

18 Human blood plasma samples were collected from the Hospital of Canakkale Onsekiz
19 Mart University in Turkey. Commercial dextrose solution (5%=277.5 mM glucose) was
20 purchased a local drugstore. The experiments related with human serum sample were
21 approved and conducted according to the guidelines of Canakkale Onsekiz Mart University
22 (Turkey) ethics committee.
23
24
25
26
27

28 3.3. Immobilization of enzyme

29
30
31 PAMAM dendrimers have attracted increasing attention in recent years because of their
32 unique structure and interesting properties. A highly branched dendritic macromolecule,
33 PAMAM, possesses a unique surface with multiple chain ends, and the number of surface
34 groups can be precisely controlled by choosing the appropriate synthetic generation. For
35 example, the fourth-generation (G4) PAMAM with a particle size of ca 5 nm possesses 64
36 surface amine groups per particle with excellent solubility in water⁴⁰. In addition, the
37 PAMAM dendrimer represents a friendly environment for the immobilization of enzymes,
38 and it is stable and capable of generating high power density compared to other
39 immobilization methods. Thus, in the enzyme immobilization procedure, G4-PAMAM was
40 used.
41
42
43
44
45
46
47

48 Prior to enzyme immobilization, GCEs were mechanically polished using a BAS-
49 polishing kit with aqueous 1.0, 0.3 and 0.05 μ m alumina (Al₂O₃) slurry on a polishing cloth
50 for three min to a mirror-like surface. After they were washed with deionized water, they were
51 cleaned by sonication in ethanol and deionized water for 5 min, respectively.
52
53
54

55 In the enzyme immobilization procedure, firstly an aliquot of 4 μ L 2 mg mL⁻¹ PAMAM
56 in methanol was cast onto the polished and cleaned bare GCE. After PAMAM was dried at
57 room temperature for about 10 min, a polymer film of HT was prepared by recording
58
59
60

1
2
3 successive (20 cycle) cyclic voltammograms of 0.3 mM HT on GCE in the potential range
4 between -0.5 and 2.0 V in the 0.1 M PBS (pH 7.0) containing 0.1 M NaNO_3 at 100 mV s^{-1} .
5 Then Poly-HT/PAMAM/GCE washed with deionized water and dried under Ar atmosphere
6 and the glucose dehydrogenase (GDH) enzyme were immobilized directly on poly-
7 HT/PAMAM/GCE by the cross-linking method using glutaraldehyde (GA). For this aim,
8 firstly 5 mg mL^{-1} GDH and 1% BSA, which were prepared in PBS, was mixed in a ratio $1:1$
9 and then 5 μL of the mixture and 4 μL of GA (20 mM) were cast on poly-HT/PAMAM/GCE,
10 respectively. Finally, this electrode was dried at 4°C in a refrigerator for at least 4 h. A
11 schematic representation of the preparation of enzyme modified electrodes is given in Figure
12 5. Enzyme was immobilized via crosslinking of aldehyde group of GA with amino groups of
13 enzyme and PAMAM (Enzyme-GA-PAMAM) in which a Schiff Bases between two amino
14 groups and aldehyde groups were produced (Enzyme- $\text{N}=\text{CH}-(\text{CH}_2)_3-\text{CH}=\text{N}-\text{PAMAM}$). Poly-
15 HT film is formed between branches of PAMAM, thus many NH_2 groups can be free for
16 crosslinking of GDH on PAMAM via GA.
17
18
19
20
21
22
23
24
25
26
27

28 **Fig. 5**

30 **3.4. Electrochemical Procedure**

31
32
33
34
35 Electrochemical and photoelectrocatalytic oxidation of glucose at this GDH based poly-
36 HT/PAMAM/GCE was investigated using cyclic voltammetric techniques. Firstly, cyclic
37 voltammogram of GDH-poly-HT/PAMAM/GCE was recorded in 0.1 M PBS (pH 7.0)
38 containing 10 mM NAD^+ in the potential range between -0.8 and 0.8 V vs. Ag/AgCl at a scan
39 rate of 5 mV s^{-1} in the absence of glucose. In order to see response of biosensor towards
40 glucose, cyclic voltammograms of modified electrodes were recorded in the same conditions
41 but in the presence of 10 mM glucose. The cyclic voltammograms in the same conditions
42 were also recorded for bare GCE, poly-HT/GCE, poly-HT/PAMAM/GCE.
43
44
45
46
47

48 Finally, photoelectrochemical biosensor studies were performed by using the home-
49 made photoelectrochemical cell¹⁶. In the photoelectrocatalytic experiments, the cyclic
50 voltammograms of GDH/poly-HT/PAMAM/GCE were recorded under the above mentioned
51 same conditions (supporting electrolyte: 0.1 M PBS (pH 7.0), scan rate: 5 mV s^{-1} , potential
52 range: from -0.8 to 0.8 V in the absence and presence of glucose), but under irradiation of the
53 working electrode surface by the fiberoptic illuminator with 250 W halogen bulb. The
54
55
56
57
58
59
60

constructed photoelectrochemical biosensor for glucose detection at GDH/poly-HT/PAMAM/GCE is schematically shown in Figure 6.

Fig. 6

3.5. Photoelectrochemical biosensor studies in FIA system

Previously constructed the new home-made photoelectrochemical flow cell and FIA diagram¹⁶ were also used for studies of electrocatalytic and photoelectrocatalytic oxidation of glucose in FIA system. In all FIA experiments, 0.1 M PBS (pH 7.0) containing 0.1 M KCl was used as carrier solution. After GDH/poly-HT/PAMAM/GCE had been inserted into a flow cell, electrochemical and photoelectrochemical responses of glucose were monitored dependent on glucose concentration. For this, after a steady-state background current of supporting electrolyte under optimum conditions, which were optimized in the FIA procedure section, was obtained, the various concentrations of glucose containing 10 mM NAD⁺ were injected into the system and the current–time curves were recorded. The current–time curves were also recorded for the photoamperometric FIA study by irradiation of electrode surface throughout experiment. In all FIA experiments, three injections were made for each NADH standard solution. Same experiments were also repeated for bare GCE for comparison. All supporting electrolytes were deaerated by allowing highly pure argon to pass through for 5 min before the electrochemical experiments.

4. Conclusion

In this study, the constructing photoelectrochemical glucose biosensor in FIA system was proposed. Although, photoelectrochemical biosensor dependent on NAD⁺/NADH redox couple-dehydrogenase enzymes^{23,24} has been reported, according to our search of the literature, photoelectrochemical biosensor in FIA system have not been reported, yet. When the electrochemical biosensor was performed, the anodic current increased linearly with the glucose concentration over the range from 1.0×10^{-5} to 1.0×10^{-3} M with the sensitivity of $0.76 \mu\text{A mM}^{-1}$ and detection limit $3.0 \mu\text{M}$. After the irradiation, the linear range of the photoelectrochemical biosensor was from 5×10^{-6} to 1.0×10^{-3} M with the sensitivity of $1.90 \mu\text{A mM}^{-1}$ and detection limit $1.5 \mu\text{M}$. Compared with the reaction without irradiation, the sensitivity and the detection limit increased around 2.5 and 2.0 folds, respectively. The

1
2
3 various analytical detection parameters such as detection potential of glucose, linearity ranges
4 and calculated LOD were compared with other modified electrodes in previously published
5 reports for the biosensing of glucose. The results are illustrated in Table 2. As can be seen, the
6 electrocatalytic detection potential of glucose (DP) at the GDH/poly-HT/PAMAM/GCE was
7 better than DP of 5-[2,5-di (thiophen-2-yl)-1H-pyrrol-1-yl]-1,10-phenanthroline iron(III)
8 chloride modified screen printed carbon electrode (SPCE). Although the DP data reported for
9 the modified electrodes were better than the GDH/poly-HT/PAMAM/GCE, the LOD and
10 linearity range of proposed electrode was better than that of the compared modified
11 electrodes.
12
13
14
15
16
17
18
19

20 As a result, this study represented the successful dehydrogenase-based electrochemical
21 and photoelectrochemical biosensors in FIA system at GDH/poly-HT/PAMAM/GCE.
22 Glucose in the commercial dextrose solution and human serum sample was successfully
23 determined with proposed electrochemical and photoelectrochemical biosensor. The
24 biocatalytical performance of the biosensor was greatly improved by the photovoltaic effect
25 of the dye using as mediator.
26
27
28
29
30

31 References

- 32 1-C. Mousty, *Anal. Bioanal. Chem.*, 2010, **396**, 315.
33
34 2-J.M. Zen, A.S. Kumar and D. Tsai, *Electroanalysis*, 2003, **15**, 1073.
35
36 3- L. Gorton, *Electroanalysis*, 1995, **7**, 23.
37
38 4- L. Gorton and E. Dominguez, *Rev. Mol. Biotechnol.*, 2002, **82**, 371.
39
40 5- S.A. Kumar and S.M. Chen, *Sensors*, 2008, **8**, 739.
41
42 6- I. Katakis and E. Dominguez, *Microchim. Acta*, 1997, **126**, 11.
43
44 7- M.J. Lobo, A.J. Miranda and P. Tunon, *Electroanalysis*, 1997, **9**, 191.
45
46 8- W.J. Blaedel and R.A. Jenkins, *Anal. Chem.*, 1975, **47**, 1337.
47
48 9- M.T. Meredith, F. Giround and S.D. Minteer, *Electrochim. Acta*, 2012, **72**, 207.
49
50 10- E. Al-Jawadi, S. Poller, R. Haddad and W. Schuhmann, *Microchim. Acta*, 2012, **177**, 405.
51
52 11- Y. Liu, H.L. Zhang, G.S. Lai, A.M. Yu, Y.M. Huang and D.Y. Han, *Electroanalysis*,
53 2010, **22**, 1725.
54
55 12- D.W. Yang and H.H. Liu, *Biosens. Bioelectron.*, 2009, **25**, 733.
56
57
58
59
60

- 1
2
3 13- P.N. Bartlett, E. Simon and C.S. Toh, *Bioelectrochem.*, 2002, **56**, 117.
4
5 14- Y. Dilgin, L. Gorton and G. Nişli, *Electroanalysis*, 2007, **19**, 286.
6
7 15- Y. Dilgin, D.G. Dilgin, Z. Dursun, H.İ. Gökçel, D. Gligor, B. Bayrak and B. Ertek,
8 *Electrochim. Acta*, 2011, **56**, 1138.
9
10 16- D.G. Dilgin, D. Gligor, H.İ. Gökçel, Z. Dursun and Y. Dilgin, *Biosens. Bioelectron.*,
11 2010, **26**, 411.
12
13 17- D.G. Dilgin, D. Gligor, H.İ. Gökçel, Z. Dursun and Y. Dilgin, *Microchim. Acta*, 2011,
14 **173**, 469.
15
16 18- D. Gligor, Y. Dilgin, I.C. Popescu and L. Gorton, *Electroanalysis*, 2009, **21**, 360.
17
18 19- K. Wang, J. Wu, Q. Liu, Y. Jin, J. Yan and J. Cai, *Anal. Chim. Acta*, 2012, **745**, 131.
19
20 20- G.L. Wang, J.J. Xu and H.Y. Chen, *Biosens. Bioelectron.*, 2009, **24**, 2494.
21
22 21- Y.H. Ho, A.P. Periasamy and S.M. Chen, *Sens. Actuators B: Chem.*, 2011, **156**, 84.
23
24 22- K. Schubert, W. Khalid, Z. Yue, W.J. Parak and Lisdat, F., *Langmuir*, 2010, **26**, 1395.
25
26 23- L. Deng, Y. Wang, L. Shang, D. Wen and F. Wang, *Biosens. Bioelectron.*, 2008, **24**, 951.
27
28 24- E.H. Hansen, *J. Mol. Recognit.*, 1996, **9**, 316.
29
30 25- M. Mayer and J. Ruzicka, *Anal. Chem.*, 1996, **68**, 3808.
31
32 26- S. Baskar, J.L. Chang and J.M. Zen, *Biosens. Bioelectron.*, 2012, **33**, 95.
33
34 27- Y. Hasebe, Y. Wang and K. Fukuoka, *J. Environ. Sci.-China*, 2011, **23**, 1050.
35
36 28- M. Piano, S. Serban, N. Biddle, R. Pittson, G.A. Drago and J.P. Hart, *Anal. Biochem.*,
37 2010, **396**, 269.
38
39 29- C. Ramirez-Molina, M. Boujtita and N. El Murr, *Electroanalysis*, 2003, **15**, 1095.
40
41 30- M.J. Lobo, A.J. Miranda and P. Tunon, *Electroanalysis*, 1996, **8**, 591.
42
43 31- A.A. Karyakin, E.E. Karyakina, W. Schuhmann and H.L. Schmidt, *Electroanalysis*, 1999,
44 **11**, 553.
45
46 32- R. Kamin and G. Wilson, *Anal. Chem.*, 1980, **52**, 1198.
47
48 33- L. Bai, D. Wen, J. Yin, L. Deng, C. Zhu and S. Dong, *Talanta*, 2012, **91**, 110.
49
50 34- R. Monosík, M. Stredansky, K. Luspai, P. Magdolend and E. Sturdík, *Enzyme Microbial*
51 *Tech.*, 2012, **50**, 227.
52
53
54
55
56
57
58
59
60

- 1
2
3 35- P. Du, P. Wu and C. Cai, *J. Electroanal. Chem.*, 2008, **624**, 21.
4
5 36- T. Hoshino S.I. Sekiguchi and H. Muguruma, *Bioelectrochem.*, 2012, **84**, 1.
6
7 37- D.M. Kim, M.Y. Kim, S.S. Reddy, J. Cho, C.H. Cho, S. Jung and Y.B. Shim, *Anal.*
8
9 *Chem.*, 2013, **85**, 11643.
10
11 38- F. Pariente, F. Tobalina, G. Moreno, L. Hernandez, E. Lorenzo and H.D. Abruna, *Anal.*
12
13 *Chem.*, 1997, **69**, 4065.
14
15 39- A.M.V. Mohan, K.K. Aswini, A.M. Starvin and V.M. Biju, *Anal. Methods*, 2013, **5**, 1764.
16
17 40- Y.L. Zeng, Y.F. Huang, J.H. Jiang, X.B. Zhang, C.R. Tang, G.L. Shen and R.Q. Yu,
18
19 *Electrochem. Commun.*, 2007, **9**, 185.
20
21 41- R. Antiochia and L. Gorton, *Biosens. Bioelectron.*, 2007, **22**, 2611.
22
23 42- F.S. Saleh, L.Q. Mao and T. Ohsaka, *Sens. Actuators B.*, 2011, **152**, 130.
24
25 43- D.M. Zhou, J.J. Sun, H.Y. Chen and H.Q. Fang, *Electrochim. Acta*, 1998, **43**, 1803.
26
27
28
29
30
31
32
33
34
35
36
37
38
39
40
41
42
43
44
45
46
47
48
49
50
51
52
53
54
55
56
57
58
59
60

Table 1. The results of recovery studies for glucose determination in real samples (n=3)

Sample	Spiked (mM)	FIA Amperometric			FIA Photoamperometric		
		Found (mM)	Recovery	RSD %	Found (mM)	Recovery	RSD %
Human serum	0.25	0.26 ± 0.01	105.2	4.0	0.26 ± 0.03	104.6	7.9
	0.50	0.49 ± 0.02	98.7	3.1	0.52 ± 0.04	103.3	7.3
	1.00	1.01 ± 0.03	101.3	2.5	1.02 ± 0.06	102.3	6.0
Dextrose solution	Labelled claim (%5=277.5 mM)	277.7 ± 4.5	-	-	282.3 ± 6.0	-	-

Table 2. Comparison of analytical parameters obtained from GDH/poly-HT/PAMAM/GCE with different electrodes in the literature for electrochemical biosensing of glucose dependent on NAD⁺/NADH redox couple and dehydrogenase enzyme.

Electrode type	Method	DP	LR	LOD	Ref.
Th cross-linked MWCNTs and Au NPs multilayer functionalized ITO electrode	AMP	0.2 V vs. Ag/AgCl	10-2560 μM	5 μM	23
	AMP under irradiation		1-3250 μM	0.7 μM	
MdB modified SPCE	FIA AMP	0.05 V vs. Ag/AgCl	75-30.000 μM	-	28
CNTs-IL/GCE	CV	0.25 V vs. Ag/AgCl	20-1000μM	9 μM	33
FAD-MWCNT nanocomposite electrode	AMP	0.05 V vs. Ag/AgCl	70-620 μM (for <i>Asp. oryzae</i>) 50-660 μM (for <i>Asp. sp</i>)	4.15 μM 4.45 μM	34
Poly-NB modified SWCNT/GCE	AMP	0.05 V vs. Ag/AgCl	10-8500 μM	5 μM	35
Au modified SWCNT-a nanothin PPF	AMP	0.2 V vs. Ag/AgCl	4900-19.000 μM	-	36
FePhenTPy modified SPCE	AMP	0.55 V vs. C electrode	30-600 mg/dL (17-330 μM)	12 mg/dL (6.7 μM)	37
CNTP modified with Os –redox polymers	AMP	0.2 V vs. Ag/AgCl	Upto 800 μM	10 μM	41
NB SWCNT modified GCE	AMP	0 V vs. SCE	100-1700 μM	0.3 μM	42
Poly-TB on graphite electrode	AMP	-	50-3000 μM	-	43
GDH/poly-HT/PAMAM/GCE	FIA AMP	0.3 V vs. Ag/AgCl	10-1000 μM	3 μM	This work
	FIA AMP under irradiation		5-1000 μM	1.5 μM	

FePhenTPy: 5-[2,5-di (thiophen-2-yl)-1H-pyrrol-1-yl]-1,10-phenanthroline iron(III) chloride, PPF: Plasma polymerized film, SPCE: Screen printed carbon electrode, LR: linearity range, DP: Detection potential, LOD: Limit of detection, CNTP: Carbon nanotube paste, AMP: Amperometry, NB: Nile Blue, SWCNT: Single walled carbon nanotube, IL Ionic liquid, TB: Toluidine blue, FAD:Flavine adenine dinucleotide, ITO: Indium tin oxide, NPs: Nanoparticles, GDH: Glucose dehydrogenase.

Figure Captions

Figure 1. Repetitive cyclic voltammograms (20 cycles) of 0.3 mM HT at PAMAM/GCE in 0.1 M PBS (pH 7.0) containing 0.1 M NaNO₃ at 100 mV s⁻¹ in the range of -0.5 to 2.1 V vs. Ag/AgCl (black and blue lines are first and last cycles, respectively).

Figure 2. Cyclic voltammograms of A) GDH/PAMAM/GCE and B) GDH/poly-HT/PAMAM/GCE in the presence of 10 mM NAD⁺ and a) in the absence, b) in the presence of 10 mM glucose without irradiation and c) b with irradiation. Supporting electrolyte: 0.1 M PBS (pH 7.0); scan rate: 5 mV s⁻¹.

Figure 3. Current-time curves of glucose with different concentrations in the range from 0.005 mM to 10 mM glucose containing 10 mM NAD⁺ using GDH/Poly-HT/PAMAM/GCE in FIA system (Carrier stream: 0.1 M PBS (pH 7.0) containing 0.1 M KCl, applied potential: 300 mV; flow rate: 0.125 mL min⁻¹; sample loop: 100 μL; transmission tubing length: 10 cm).

Figure 4. A) Dependence of the catalytic currents on glucose concentration, B) calibration curve for ■) amperometric and ●) photoamperometric analysis of glucose using GDH/Poly-HT/PAMAM/GCE in FIA system.

Figure 5. Schematic representation of enzyme immobilization procedure.

Figure 6. Schematic representation of the photoelectrochemical biosensor.

Figure 1

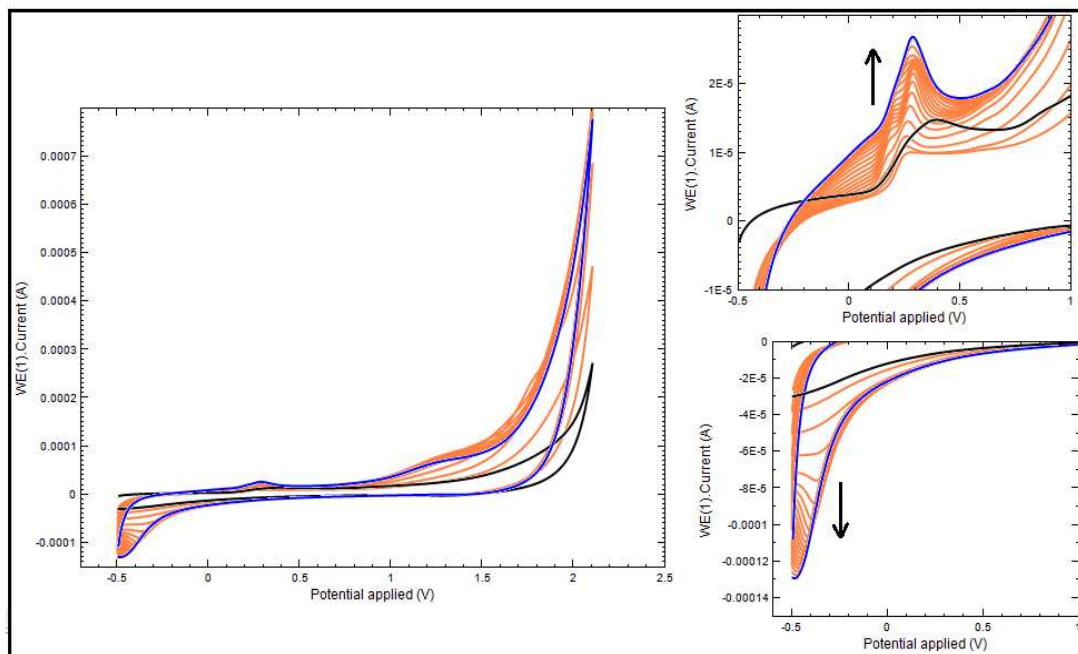


Figure 2

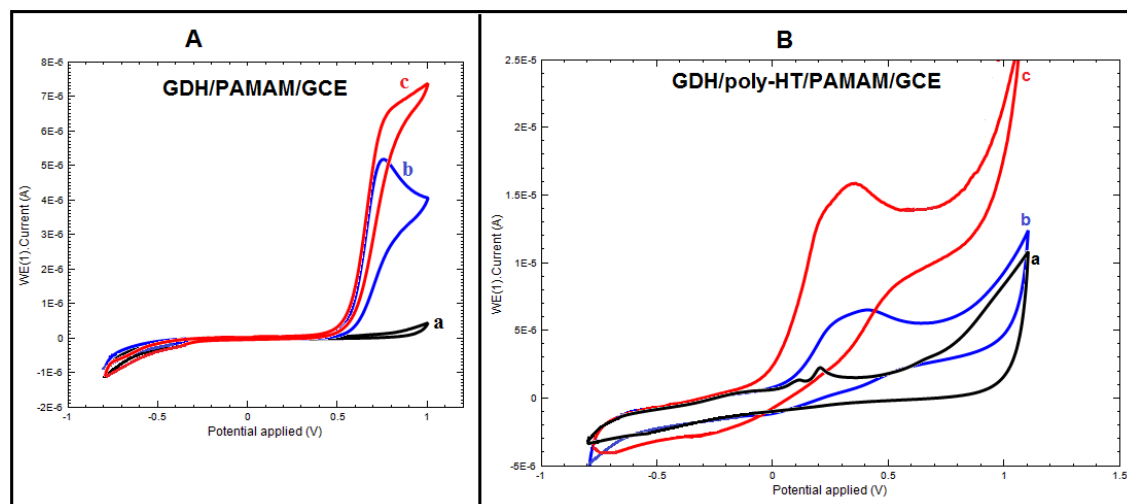
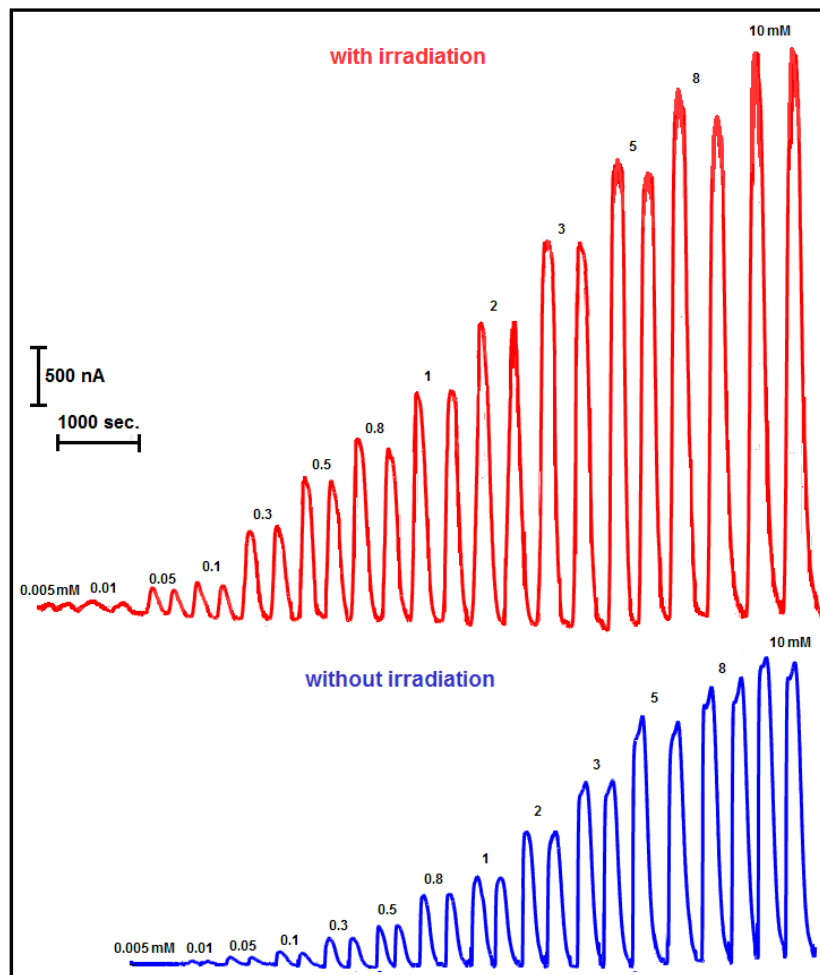


Figure 3



1
2
3
4
5
6
7
8
9
10
11
12
13
14
15
16
17
18
19
20
21
22
23
24
25
26
27
28
29
30
31
32
33
34
35
36
37
38
39
40
41
42
43
44
45
46
47
48
49
50
51
52
53
54
55
56
57
58
59
60

Figure 4

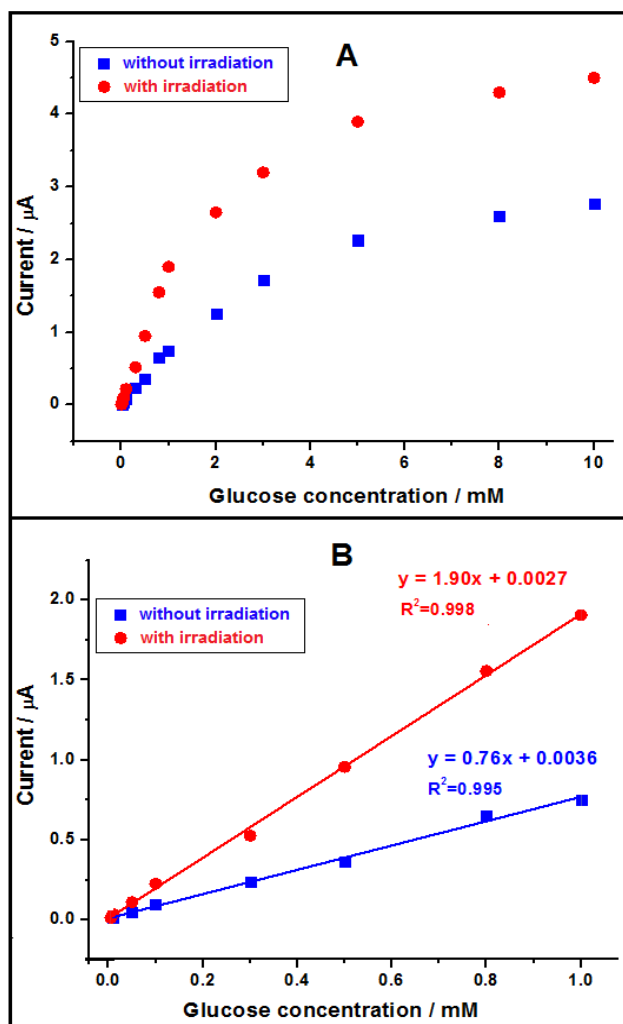
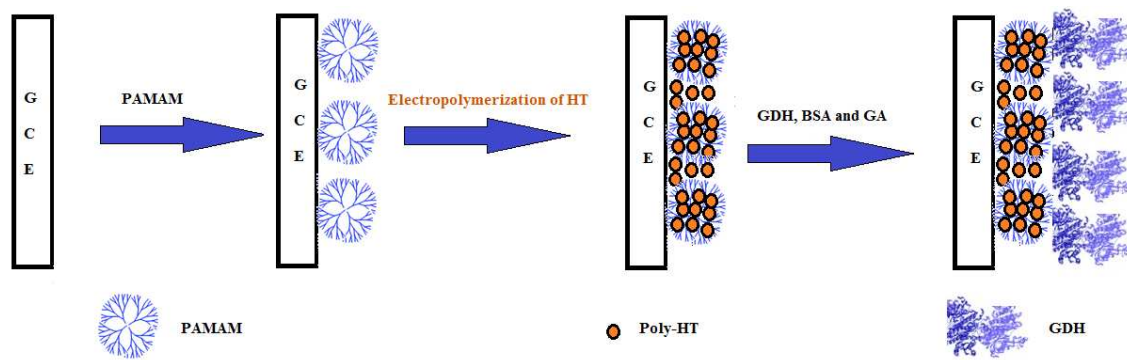
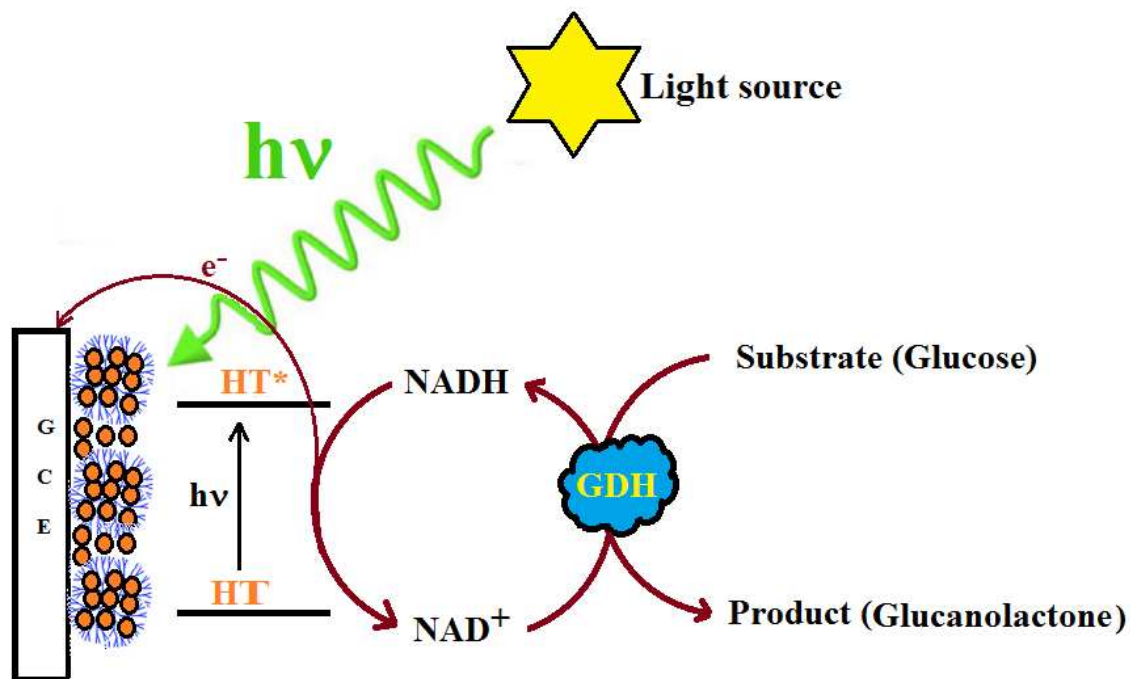


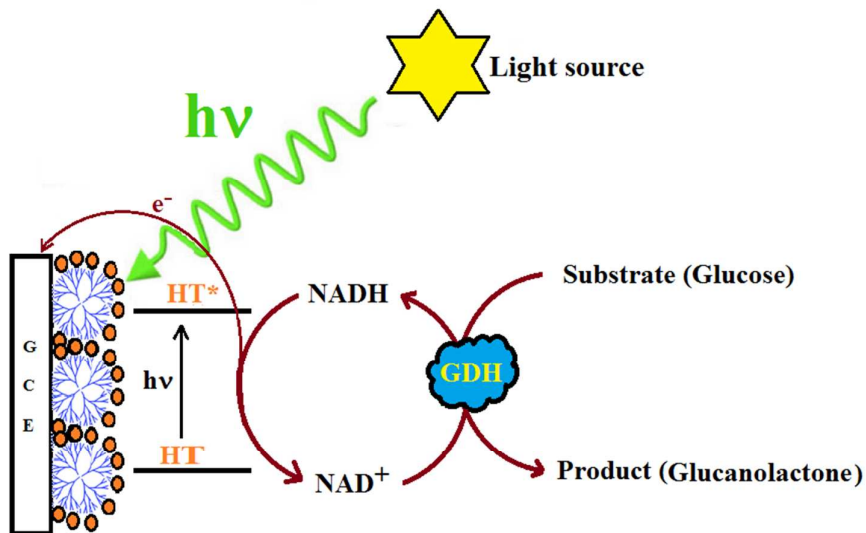
Figure 5



1
2
3
4
5
6
7
8
9
10
11
12
13
14
15
16
17
18
19
20
21
22
23
24
25
26
27
28
29
30
31
32
33
34
35
36
37
38
39
40
41
42
43
44
45
46
47
48
49
50
51
52
53
54
55
56
57
58
59
60

Figure 6





1
2
3
4
5
6
7
8
9
10
11
12
13
14
15
16
17
18
19
20
21
22
23
24
25
26
27
28
29
30
31
32
33
34
35
36
37
38
39
40
41
42
43
44
45
46
47
48
49
50
51
52
53
54
55
56
57
58
59
60